

Shell model description of “mixed-symmetry” states in ^{94}Mo

A. F. Lisetskiy¹, N. Pietralla^{1,2}, C. Fransen¹, R. V. Jolos^{1,3}, P. von Brentano¹

¹ *Institut für Kernphysik, Universität zu Köln, 50937 Köln, Germany*

² *Wright Nuclear Structure Laboratory, Yale University, New Haven, CT 06520-8124*

³ *Bogoliubov Theoretical Laboratory, Joint Institute for Nuclear Research,*

141980 Dubna, Russia

(November 18, 2018)

Abstract

Shell model calculations have been performed for the nucleus ^{94}Mo . The calculated excitation energies and electromagnetic properties of low-lying states are in good agreement with the data, which include states with mixed-symmetry (MS) assignments in previous Interacting Boson Model studies. In the shell model large isoscalar $E2$ matrix elements are found between states with MS assignments indicating that they form a class of states with similar proton-neutron symmetry.

Keywords: Shell model, ^{94}Mo , mixed symmetry states.

I. INTRODUCTION

Recently performed photon scattering experiments and $\gamma\gamma$ -coincidence studies [1,2] of the nucleus ^{94}Mo indicate the existence of low-lying valence shell excitations with proton-neutron symmetry different to that of the ground state in that nucleus. The measurements [1,2] of absolute $E2$ and $M1$ transition strengths have been interpreted in terms of $J^\pi = 1^+, 2^+, 3^+$ mixed-symmetry states in the framework of the proton-neutron version [3] of the Interacting Boson Model (IBM-2). The proton-neutron symmetry of an IBM-2 wavefunction is quantified by the F -spin quantum number [3,4], which is the isospin for basic proton and neutron bosons. The IBM-2 predicts the lowest-lying collective states to be dominantly isoscalar excitations of the almost proton-neutron symmetric ground state with maximum F -spin quantum number $F = F_{\max}$. This is put in evidence by the existence of F -spin multiplets with rather constant energies [5]. The IBM-2 predicts also valence shell excitations with wavefunctions, which are not symmetric with respect to the proton-neutron degree of freedom [3,4,6,7]. Such states have F -spin quantum numbers $F < F_{\max}$ and are called *mixed-symmetry* (MS) states. The observations for the $1_1^+, 2_3^+, 3_2^+$ states of ^{94}Mo agree with MS assignments [1,2]. The key-signatures used for the assignments of MS character to these states of ^{94}Mo were the measured relatively strong $M1$ transitions and weakly-collective $E2$ transitions to low-lying symmetric states.

Separate proton and neutron quadrupole surface vibrations, which lead to eigenstates with different symmetries with respect to proton-neutron permutations, have been considered in a geometrical model already in the sixties by Faessler [8]. At that time these states were predicted to exist above the particle threshold, at a much higher energy than recently observed. In the eighties [9,10] the isovector vibrational model was improved giving quantitatively better description of the 2^+ isovector vibrational states. The existence of collective orbital isovector $M1$ transitions in the geometrical Two Rotor Model for deformed nuclei was realized by Lo Iudice and Palumbo [11]. A more general type of enhanced magnetic dipole transitions in the valence shell of all open-shell nuclei, not only deformed, has been predicted [3,4,6,7] in the IBM-2 as the decays of MS states. Following these predictions the dominantly isovector $J^\pi = 1^+$ state, generally called scissors mode, was discovered by Richter *et al.* [12] in inelastic electron scattering experiments in Darmstadt. The typically fragmented 1_{sc}^+ scissors mode was further investigated mainly by electron scattering [13], photon scattering [14] and neutron scattering [15] experiments.

Many theoretical studies were published to explain the structure of this mode, e.g. [16–22]. The 1^+ mode is expected to be dominantly excited by the isovector part of the $M1$ operator indicating its isovector character. The large $M1$ transition strength and its close correlation [23–26] to the collective $E2$ excitation strength in deformed nuclei is usually considered an indication of the collective nature of the 1_{sc}^+ state. Another state with spin different from $J^\pi = 1^+$ but of similar isovector character, the one-quadrupole phonon 2_{ms}^+ state, has been identified from $M1$ strengths, too. The first 2_{ms}^+ assignments to states at about 2 MeV in vibrational nuclei around the $N = 82$ shell closure were based only on small $E2/M1$ multipole mixing ratios [27–30]. Later on, several of these assignments were confirmed by the measurement of relatively large $M1$ and weakly-collective $E2$ transition

strengths [31–34]. Based on measured $M1$ and $E2$ strengths the experimentally observed 1_1^+ , 2_3^+ , and 3_2^+ states in the nucleus ^{94}Mo were argued to belong to this type of excitations, too [1,2].

In nuclei not too far from shell closures the structure of low-lying valence excitations including the states, which are outside of the IBM configurational space, can be described using the shell model. It is the main aim of the present paper to describe the structure of the states observed in [1,2] in the framework of the nuclear shell model, especially the structure of the 1_1^+ , 2_3^+ and 3_2^+ states. We present the results of shell model calculations for the low-lying positive parity states of ^{94}Mo with spin quantum numbers $J^\pi = 0^+ - 4^+$ and we discuss the isotensor character of their electromagnetic transitions.

II. THEORETICAL APPROACH

The shell model Hamiltonian is taken as $H = H_0 + V$ where the mean field is given by

$$H_0 = \sum_k^{n_{\text{val}}} \varepsilon_k a_{\rho_k}^+ a_{\rho_k}, \quad (1)$$

where n_{val} is a number of single particle states in the adopted valence shells and the residual interaction is

$$V = \sum_{\rho_a, \rho_b, \rho_c, \rho_d, J, M, T} <(\rho_a \rho_b)_{JT}|V_{12}|(\rho_c \rho_d)_{JT}> (a_{\rho_a}^+ a_{\rho_b}^+)^T_{JM} (a_{\rho_c} a_{\rho_d})^T_{JM}. \quad (2)$$

Here a_ρ^+ creates and a_ρ annihilates a particle in the single particle orbital $|\rho\rangle \equiv |n, l, j, m_j, t = 1/2, t_z\rangle$ and T is the isospin of the coupled particles. The first term H_0 is the Hamiltonian of the noninteracting particles. The residual interaction we used is the Surface Delta Interaction (SDI) [35]. This interaction contains strong pairing and quadrupole parts and higher multipolarity components, which are weaker than the first two. The SDI is an extremely simple interaction from the mathematical point of view. The two body matrix elements of the SDI are:

$$<\rho_a \rho_b | V_{SDI}(\mathbf{r}_1, \mathbf{r}_2) | \rho_c \rho_d>_{JT} = -4\pi A'_T <\rho_a \rho_b | \delta(\Omega_{12}) \delta(r_1 - R) \delta(r_2 - R) | \rho_c \rho_d>_{JT} \quad (3)$$

where Ω_{12} is the angle between the interacting particles, $R = 1.2 A^{1/3}$ fm is the nuclear radius, and A'_T is the strength constant of the SDI. There are three parameters $A'^{\rho', \rho}_{T=1}$ ($\rho, \rho' \in \{p, n\}$) that describe the interaction in the $T=1$ channel and one parameter $A'^{pn}_{T=0}$ describing the interaction in the $T=0$ channel. The fitted interaction parameters $A'^{\rho', \rho}_T$ are connected to the parameters from Eq.(3) by the following expression: $A'^{\rho', \rho}_T = A'^{\rho', \rho}_T <\delta(r_\rho - R) \delta(r_{\rho'} - R)>$, where the radial matrix elements $<\delta(r_\rho - R) \delta(r_{\rho'} - R)>$ are supposed to be independent of the single particle states involved (see for details [36]).

For the shell model description of ^{94}Mo one may want to consider the $N = Z = 50$ closed shell nucleus ^{100}Sn as the inert core. In order not to have to treat a too large model space we consider eight proton holes in the proton shells $\pi g_{9/2}$ and $\pi p_{1/2}$ for the description of $^{94}_{42}\text{Mo}$. Because of the Pauli principle this problem is equivalent to the consideration of four proton particles in these shells outside of the core $^{88}_{38}\text{Sr}_{50}$. Therefore, we adopt ^{88}Sr as the inert core for the following shell model description of ^{94}Mo .

Single-particle energies ε_j were obtained from calculations for the neutron-odd nuclei ^{89}Sr , ^{91}Zr and ^{93}Mo and for the proton-odd nuclei ^{89}Y , ^{91}Y , ^{91}Nb , ^{93}Nb , and ^{93}Tc . These single-particle energies are close to those from [37]. In order to get a rough estimate of the values of $A_{T=1}^{nn}$ and $A_{T=1}^{pp}$ parameters shell model calculations have been performed for the isobars ^{90}Sr and ^{90}Zr , which have either 2 neutrons or 2 protons, respectively, outside the core ^{88}Sr (see Fig.1). The results are $A_{T=1}^{nn} = 0.23$ MeV and $A_{T=1}^{pp} = 0.35$ MeV. The $A_{T=1}^{pn}$ parameter is taken as the average of $A_{T=1}^{nn}$ and $A_{T=1}^{pp}$, i.e. $A_{T=1}^{pn} = (A_{T=1}^{nn} + A_{T=1}^{pp})/2$. The value of 0.48 MeV for the $A_{T=0}^{pn}$ parameter was obtained by a fit to the excitation energies of the nucleus ^{92}Zr , which contains 2 protons and 2 neutrons outside the core ^{88}Sr . Experimental and calculated low-spin level schemes for the three even-even nuclei ^{90}Sr , ^{90}Zr , and ^{92}Zr are shown in Fig.1. The final values of the SDI parameters used for the description of ^{94}Mo were optimized by a fit to the low-spin level scheme of ^{94}Mo and are close to the values above. It is interesting to note that the excitation energies of low-lying states are much less sensitive to the $A_{T=1}^{pn}$ parameter than to the $A_{T=0}^{pn}$ parameter. However the electromagnetic transition strengths are very sensitive to both $A_{T=1}^{pn}$ and $A_{T=0}^{pn}$ parameters and the above discussed choice gives the best agreement between calculated and experimental strengths in ^{94}Mo nucleus. The single-particle energies and SDI parameters used for ^{94}Mo are presented in Table I. The SM calculations were performed on the Cologne Sun Ultra Enterprise 4000 workstation with two 166 MHz Ultra Sparc processors using the code RITSSCHIL [38].

III. DISCUSSION

In the present shell model calculation for ^{94}Mo two neutrons can be distributed among five single particle orbitals: $2d_{5/2}$, $3s_{1/2}$, $1g_{7/2}$, $2d_{3/2}$ and $1h_{11/2}$. The lowest neutron orbital is $2d_{5/2}$. The fully occupied neutron orbital $1g_{9/2}$ forms the $N = 50$ closed shell and is about 4 MeV below the neutron $2d_{5/2}$ orbital. Therefore, the influence of the $1g_{9/2}$ orbital on the structure of low-lying states of ^{94}Mo is expected to be small¹. This justifies the assumption of the $N = 50$ neutron core. For protons we have included the two orbitals $1g_{9/2}$ and $2p_{1/2}$ in the configurational space. The closest higher-lying proton orbital to the proton $1g_{9/2}$ orbital appears more than 4 MeV above the $Z=50$ closed shell and is neglected. But the proton $p_{1/2}$ orbital is much closer to the proton $1g_{9/2}$ – about 1 MeV lower – and we have taken it into account by choosing $Z = 38$ as the proton core. Within this configurational space we reproduce well many of the excited states in the spectrum of ^{94}Mo . This is shown in Fig. 2.

The main components of the low-lying states (see Table II) are seniority 2 and 4 with two protons in $\pi(1g_{9/2})$ and two neutrons in $\nu(2d_{5/2})$. But the influence of the $\pi(2p_{1/2})$ proton orbital is also significant - almost all states contain large components $\pi(p_{1/2}^{-2}g_{9/2}^4)_J$ and this is the main component for the 0_2^+ state. The contributions of the neutron orbitals $\nu(3s_{1/2})$, $\nu(1g_{7/2})$, $\nu(2d_{3/2})$ and $\nu(1h_{11/2})$ are smaller but for the 1_2^+ the component $\nu(g_{7/2}^1d_{5/2}^1)$ is already the main one.

¹This expectation is supported by the first results of large scale shell model calculations for ^{94}Mo assuming the $Z = N = 40$ nucleus ^{80}Zr as the inert core, which yield at the present stage almost negligible contributions of the $\nu(g_{9/2})$ orbital to low-lying low-spin states of ^{94}Mo [39].

The $M1$ and $E2$ transition probabilities have been calculated and compared with the new experimental data. The results are shown in Tables III and IV. The reproduction of the data is in most cases very good. Tables III and IV include also IBM-2 predictions in the $O(6)$ dynamical symmetry limit, where the states $1_1^+, 2_3^+, 3_2^+$ have mixed-symmetry. We note that the IBM-2 has only one free parameter - the effective quadrupole proton boson charge e_p , while the corresponding neutron charge was put to zero $e_n = 0$. It is remarkable how well the shell model agrees also with the IBM-2 with only a few exceptions. The agreement of shell model calculations with IBM-2 results in different mass regions was noted also by other authors (see, for instance, [40,41]).

Let us discuss now the calculated $M1$ and $E2$ transition strengths in more detail. The MS assignments for the $1_1^+, 2_3^+, 3_2^+$ states of ^{94}Mo were based on the measurements of relatively large $M1$ transition strengths. For the calculation of $M1$ transitions between the shell model states we consider a nuclear magnetic dipole operator, which is the sum of proton and neutron one-body terms for orbital and spin contributions:

$$\mathbf{T}(M1) = \sqrt{\frac{3}{4\pi}} \left(\sum_{i=1}^Z [g_p^l \mathbf{l}_i^p + g_p^s \mathbf{s}_i^p] + \sum_{i=1}^N [g_n^l \mathbf{l}_i^n + g_n^s \mathbf{s}_i^n] \right) \mu_N, \quad (4)$$

where g_ρ^l and g_ρ^s are the orbital and spin g-factors and $\mathbf{l}_i^\rho, \mathbf{s}_i^\rho$ are the single particle orbital angular momentum operators and spin operators. For further discussion it is useful to decompose the $M1$ operator into an isoscalar part

$$\mathbf{T}_{IS}(M1) = \sqrt{\frac{3}{4\pi}} (g_J \mathbf{J} + g_S \mathbf{S}) \mu_N, \quad (5)$$

and an isovector part

$$\mathbf{T}_{IV}(M1) = \sqrt{\frac{3}{4\pi}} \left(\frac{g_p^l - g_n^l}{2} [\mathbf{L}_p - \mathbf{L}_n] + \frac{g_p^s - g_n^s}{2} [\mathbf{S}_p - \mathbf{S}_n] \right). \quad (6)$$

where \mathbf{L}_ρ and \mathbf{S}_ρ denote the total orbital angular momentum and total spin operators for protons ($\rho = p$) and neutrons ($\rho = n$). $\mathbf{J} = \mathbf{L} + \mathbf{S}$ is the total angular momentum and does not generate $M1$ transitions. $g_J = (g_p^l + g_n^l)/2 = 1/2$ and $g_S = [g_p^s + g_n^s - (g_p^l + g_n^l)]/2 = 0.88\alpha_q - 1/2$ with the quenching factor α_q defined by $g_\rho^s = \alpha_q g_\rho^{s,\text{free}}$. The free spin g-factors are $g_p^{s,\text{free}} = 5.58$ and $g_n^{s,\text{free}} = -3.82$. Since g_p^s and g_n^s are of opposite sign and comparable, the isoscalar nondiagonal piece of an $M1$ matrix element is usually very small. It vanishes exactly for a quenching factor $\alpha_q = 0.57$. For a good reproduction of the measured $M1$ transition strengths (see Table III) and for the sake of easy interpretation we used the quenching factor $\alpha_q = 0.57$ which results in pure isovector $M1$ transitions.

The isovector $M1$ ground state excitation strength is calculated to be concentrated in the 1_1^+ state. This agrees with the identification of the 1_1^+ state with the scissors mode in the nucleus ^{94}Mo . This identification receives further support from the consistency [1] of the data on ^{94}Mo with the systematics of the scissors mode extrapolated from the deformed rare earth nuclei. However, one cannot ascribe the collective scissor mode in the near-spherical nucleus ^{94}Mo as a pure orbital mode. Our calculations show that spin and orbital contributions are almost equal which agrees with the results of a single j shell model [42].

The key signature for the lowest 2_{ms}^+ state, with a proton-neutron symmetry similar to that of the scissors mode, is a strong $M1$ transition to the 2_1^+ state. Therefore, it is interesting to look to the $2_1^+ \rightarrow 2_i^+$ $M1$ strength distribution to judge the possible fragmentation of the 2_{ms}^+ state. From the data it follows that the $2_3^+ \rightarrow 2_1^+$ is the strongest $M1$ transition from an excited 2^+ state to the 2_1^+ state which led to the MS assignment for the 2_3^+ state. Comparing the calculated $M1$ strengths of the $2_2^+ \rightarrow 2_1^+$, $2_3^+ \rightarrow 2_1^+$ and $2_4^+ \rightarrow 2_1^+$ transitions one notes that the calculated $B(M1; 2_3^+ \rightarrow 2_1^+)$ value is about five times larger than the other two. The dominance of the $B(M1; 2_3^+ \rightarrow 2_1^+)$ value agrees with the data. The calculated $B(M1; 2_3^+ \rightarrow 2_1^+)$ value is also more than four times larger than the calculated $B(M1; 2_5^+ \rightarrow 2_1^+)$ value, which already overestimates the data. The shell model calculation agrees with the observation that the $2_3^+ \rightarrow 2_1^+$ transition concentrates the $M1$ strength between excited 2^+ states and the 2_1^+ state. This relatively strong isovector $M1$ transition agrees with the MS assignment for the 2_3^+ state.

Also the experimental 3_2^+ state decays by relatively strong $M1$ transitions to low-lying states. The calculated excitation energy of the 3_2^+ state matches the experimental energy within 50 keV whereas the 3_1^+ state lies 120 keV lower and the 3_3^+ state lies 350 keV higher than the experimental 3_{ms}^+ state. Therefore we compare the 3_2^+ shell model state with the observed 3_2^+ state at 2965 keV. We note that the measured strong $M1$ transition from the 3_2^+ state to the 4_1^+ state is reproduced by the shell model within the experimental error bar. The shell model, however, underestimates the $M1$ strength of the $3_2^+ \rightarrow 2_2^+$ transition by a factor of two, while it overestimates the $3_2^+ \rightarrow 2_1^+$ $M1$ transition strength by an order of magnitude. The shell model results for the 3_2^+ state disagree not only somewhat with the data but also with the prediction of the IBM in the O(6) dynamical symmetry limit for the 3_{ms}^+ state. However, the 3_1^+ and 3_2^+ states are close in energy, which renders the calculation of the wave functions more uncertain in the shell model, where no quantum number like the F -spin exists, which can assure the orthogonality of MS states to symmetric states. Moreover, the calculated 3_3^+ state also shows $M1$ and $E2$ properties which are close to those of the experimental 3_{ms}^+ state. We conclude that the 3_{ms}^+ character is spread about the first three 3^+ states in our shell model calculation with the surface delta residual interaction and the ^{88}Sr core. Thus for the 3_2^+ state the MS assignment from the shell model results is less clear. We consider this fact not as an argument against the MS assignment of the experimental 3_2^+ state of ^{94}Mo but as an indication of the limit of our present shell model approach for the description of the details (and the mixing) of wave functions for states, which lie close in energy. In total the $M1$ transition strengths calculated in the shell model support (or at least do not disagree with) the MS assignments for the 1_1^+ , 2_3^+ , and 3_2^+ states of ^{94}Mo , if the existence of relatively strong isovector $M1$ transition is considered as a sufficient argument in favor of MS structures.

However, it should be stressed that the strongest $M1$ transition found in ^{94}Mo nucleus [44] connects the 4_2^+ and 4_1^+ states that is in agreement with the present shell model calculations. This transition falls out from the sd -IBM-2 scheme and probably is related to the excitations of g -bosons in terms of the IBM.

Having found support for MS assignments from the large isovector $M1$ transition strengths it is interesting to turn to the $E2$ transition properties. While the existence of large isovector $M1$ transitions may indicate a different proton-neutron symmetry, one can, in contrast, judge a similar proton-neutron symmetry for two states from the existence of

collective isoscalar $E2$ transition matrix elements between the two states. The $E2$ transition operator is the sum of proton and neutron parts:

$$\mathbf{T}(E2) = e_p \mathbf{T}_p(E2) + e_n \mathbf{T}_n(E2), \quad (7)$$

where e_p and e_n are the proton and the neutron effective quadrupole charges and $\mathbf{T}_\rho(E2) = \sum_i (r_i^\rho)^2 \mathbf{Y}_2(\theta_i^\rho, \phi_i^\rho)$. It is again convenient to decompose the $E2$ operator in an isoscalar part

$$\mathbf{T}_{IS}(E2) = \frac{e_p + e_n}{2} [\mathbf{T}_p(E2) + \mathbf{T}_n(E2)], \quad (8)$$

and in an isovector part

$$\mathbf{T}_{IV}(E2) = \frac{e_p - e_n}{2} [\mathbf{T}_p(E2) - \mathbf{T}_n(E2)]. \quad (9)$$

The calculated $E2$ transition strengths and matrix elements are compared to experiment and to schematic IBM-2 estimates in Tab. IV. In the low-lying low-spin level scheme of ^{94}Mo one expects from a simple quadrupole vibrator picture the existence of the collective isoscalar $E2$ transitions which are indicated in Fig. 3. The transition from the 2_1^+ state to the 0_1^+ ground state is a collective isoscalar $E2$ transition. Many components of the wave function of the 2_1^+ state contribute coherently to the matrix element of the $E2$ transition operator. The isoscalar part of the $\langle 2_1^+ \parallel E2 \parallel 0_1^+ \rangle$ matrix element is about ten times larger than the isovector part (see most right columns of Table IV). This is a well known general property of the lowest collective 2^+ state. For ^{94}Mo the 2_1^+ state is calculated to exhaust 97% of the total isoscalar $E2$ excitation strength of the ground state to the 2^+ states up to 4 MeV. The $4_1^+ \rightarrow 2_1^+$ and $2_2^+ \rightarrow 2_1^+$ transitions are of similarly collective dominantly isoscalar $E2$ character. The strong collective isoscalar $E2$ transitions between the 0_1^+ , 2_1^+ , 4_1^+ and 2_2^+ states prove the proton-neutron symmetry of these states.

The $E2$ transitions from the 2_2^+ state and the 2_3^+ state to the ground state are much weaker than the $2_1^+ \rightarrow 0_1^+$ transition. The $2_2^+ \rightarrow 0_1^+$ transition has isovector character but it is weak. The 2_3^+ state, however, carries 10% of the total $E2$ excitation strength of the 2_1^+ state and it is the largest $E2$ excitation above the 2_1^+ state. This supports the one-phonon character of the 2_3^+ state, which is suggested from its interpretation as the one-quadrupole phonon 2_{ms}^+ state. Indeed, the transition from the 2_3^+ state to the ground state is a mixture of isoscalar and isovector parts with a notable isovector component.

The $E2$ matrix elements *between* various states with MS assignments are very interesting. The calculated wave functions of the 1_1^+ state and the 3_2^+ state are dominated by basis states with seniority $\nu = 4$ supporting their two-phonon interpretation. The 1_1^+ state shows no collective $E2$ transitions to the 2_1^+ , 2_2^+ states. The $1_1^+ \rightarrow 2_3^+$ transition is in contrast a collective isoscalar $E2$ transition which is comparable in strength with the $2_1^+ \rightarrow 0_1^+$ collective $E2$ transition. This indicates a similar proton-neutron symmetry of the 1_1^+ state and the 2_3^+ state and justifies to consider the 1_1^+ state a two-phonon state formed by an isoscalar quadrupole phonon built on top of the MS 2_3^+ state. The 2_3^+ state has a proton-neutron symmetry similar to the 1_1^+ state, but it is lower in energy and is of seniority $\nu = 2$ like the collective lowest 2_1^+ state. Also the calculated 3_2^+ state decays by a strong collective isoscalar $E2$ transition to the 2_3^+ state. The calculated $3_2^+ \rightarrow 2_1^+$ $E2$ transition strength is five times smaller than the $3_2^+ \rightarrow 2_3^+$ transition strength and the isovector part of the $E2$

matrix element is larger than the isoscalar part. Based on this comparison we can conclude that the 3_2^+ state has qualitatively a similar proton-neutron symmetry as the 1_1^+ state and the 2_3^+ states. This conclusion supports the statement that the 3_2^+ state of ^{94}Mo is one more representative of proton-neutron collective states with a “mixed-symmetry” character as it was argued before in Ref. [2]. We note, that also the calculated $3_2^+ \rightarrow 2_2^+ E2$ transition has a large isoscalar part, which, however, overestimates the data. This disagreement may again be caused by a too large mixing of the calculated 3_1^+ and 3_2^+ states and is probably due to a too large symmetric three-phonon component in the calculated wave function of the 3_2^+ state.

Of particular interest in this article is the proton-neutron structure of those states to which mixed-symmetry was previously assigned from the measurements of large $M1$ and $E2$ transition strengths [1,2]. In order to simplify the discussion we consider now a schematic model for the analysis of the wave function of the 2_{ms}^+ state, which reflects the logic of the IBM-2. Let us assume that valence protons and neutrons couple separately to collective $J_\rho^\pi = 2_p^+$ and $J_\rho^\pi = 2_n^+$ configurations with seniorities $\nu = 2$. In a two-level model one collective 2_s^+ state is formed by symmetric linear combination of the 2_p^+ proton and 2_n^+ neutron configurations: $|2_s^+ \rangle = (|2_p^+ \rangle + |2_n^+ \rangle)/\sqrt{2}$. The orthogonal linear combination $|2_{ns}^+ \rangle = (|2_p^+ \rangle - |2_n^+ \rangle)/\sqrt{2}$ has also seniority $\nu = 2$ and is the collective “nonsymmetric” counterpart of the $|2_s^+ \rangle$ state. Furthermore, the 2_p^+ proton and 2_n^+ neutron configurations can couple to collective $J^\pi = 1^+, 3^+$ states with seniority $\nu = 4$ and isovector character of decay to the 2_s^+ state. The last three states should correspond to the lowest $1^+, 2^+, 3^+$ MS states in the IBM-2. The possible existence of such states in ^{94}Mo and in neighboring nuclei as a result of quadrupole surface vibrations in anti-phase and corresponding two-phonon excitations was discussed earlier in a geometrical approach by A. Faessler [8].

In the realistic shell model calculation for ^{94}Mo presented above MS states cannot so easily be identified from the wave functions. Isospin symmetry and seniority conservation are broken due to the interaction chosen and the single particle orbitals considered. The ground state contains 72% components with seniority $\nu = 0$. The 2_1^+ and 2_3^+ states contain 70 % and 73 % components of seniority $\nu = 2$. The relatively large components with seniority $\nu = 2$ point at their predominantly one-quadrupole phonon nature [43,1]. In contrast, the wave function of the 2_2^+ state contains a large component of seniority $\nu = 4$ (50% of the wave function) in agreement with its usual two-quadrupole phonon interpretation.

Let us now further analyze the calculated wave functions of the 2_1^+ state and the 2_3^+ state, which are considered to represent well the symmetric and the MS one-phonon 2^+ states of the IBM-2. It is interesting that the components of the $2_{1,3}^+$ states with seniority $\nu = 2$, $|2_1^+, \nu = 2\rangle$ and $|2_3^+, \nu = 2\rangle$, are approximately orthogonal. Their normalized scalar product

$$\frac{\langle 2_1^+, \nu = 2 | 2_3^+, \nu = 2 \rangle}{\sqrt{\langle 2_1^+, \nu = 2 | 2_1^+, \nu = 2 \rangle \times \langle 2_3^+, \nu = 2 | 2_3^+, \nu = 2 \rangle}} = -0.07$$

is small. This fact is not a trivial consequence of the orthogonality of the $|2_3^+\rangle$ and $|2_1^+\rangle$ eigenstates, because their wave functions contain noticeable components with higher seniority. The seniority $\nu=2$ components resemble the schematic symmetric $|2_s^+\rangle$ and “nonsymmetric” $|2_{ns}^+\rangle$ states discussed above and can be used for further analysis. For this purpose it is interesting to decompose the seniority $\nu=2$ components of the 2_1^+ and 2_3^+ states into their proton and neutron parts. One obtains

$$|2_1^+, \nu = 2\rangle = 0.61|2_{1,p}^+\rangle + 0.80|2_{1,n}^+\rangle \quad (10)$$

and

$$|2_3^+, \nu = 2\rangle = 0.56|2_{3,p}^+\rangle - 0.82|2_{3,n}^+\rangle. \quad (11)$$

These decompositions cannot be directly compared to the schematic two level model mentioned above, because the basis states $|2_{i,\rho}^+\rangle$ are not identical. It turns out, however, that the normalized proton $|2_{3,p}^+\rangle$ basis state is rather similar to the normalized $|2_{1,p}^+\rangle$ basis state with a positive overlap of $\langle 2_{3,p}^+ | 2_{1,p}^+ \rangle = 0.98$. However, the overlapping of the neutron components of the states (10) and (11) is smaller. It amounts only to $\langle 2_{3,n}^+ | 2_{1,n}^+ \rangle = 0.63$ indicating considerable deviations from the pure IBM-2 picture. For a direct comparison between the structure of the $|2_i^+, \nu = 2\rangle$ components it is more useful to express the components $|2_{3,\rho}^+\rangle$ in Eq. (11) by a linear combination of one part which is parallel to the $|2_{1,\rho}^+\rangle$ components and an orthogonal rest term $|R\rangle$ with $\langle R | 2_{1,\rho}^+ \rangle \equiv 0$. We obtain

$$|2_3^+, \nu = 2\rangle = \gamma [0.72|2_{1,p}^+\rangle - 0.68|2_{1,n}^+\rangle] + |R\rangle \quad (12)$$

This result can be interpreted in the following way: The dominant seniority $\nu = 2$ component of the 2_3^+ state contains a fraction of $\gamma^2 = 58\%$ of components that form the dominant seniority $\nu = 2$ component of the 2_1^+ state. Moreover, this fraction is almost orthogonal to the seniority $\nu = 2$ component of the 2_1^+ state, because the proton part and the neutron part contribute with a different sign while their amplitudes are almost equal. Based on this observation one can consider the $|2_3^+\rangle$ state as a good realization of the collective $|2_{\text{ms}}^+\rangle$ MS state.

The schematic analysis given above helps to make some more general conclusions about the nuclear structure properties which can lead to the appearance of the “mixed symmetry” states in near-spherical nuclei. At first, we remind that the amplitudes of proton and neutron parts of symmetric and nonsymmetric states have to be approximately equal. These proton (neutron) parts of the wave functions of the symmetric state and its nonsymmetric counterpart must be rather similar, too. As it follows from our calculations this condition can be achieved if the configurational space for valence protons (neutrons) may be restricted to one high-j orbital (in our case proton $1g_{9/2}$) and one of the nearest orbitals with small single particle j quantum number (in our case proton $2p_{1/2}$). An ideal case is a single high-j orbital. Otherwise, if there are few neighboring neutron (proton) orbitals with the j value comparable to the single particle angular momentum of the selected leading neutron (proton) orbital and if the influence of these orbitals cannot be neglected, then the neutron (proton) parts of the symmetric and nonsymmetric states can be rather different. We can observe it already in our case for the neutron parts of the 2_1^+ state and the 2_3^+ state: the overlapping $\langle 2_{3,n}^+ | 2_{1,n}^+ \rangle$ is only 0.63. Therefore it can be expected that with the increase of the number of valence neutrons in the considered configurational space the neutron parts will be stronger fragmented and the neutron overlapping can be significantly reduced destroying the picture. On the contrary the increase of the number of valence protons in $1g_{9/2}$ orbital will keep the proton parts similar and the “mixed symmetry” 2^+ state will probably survive. We hope that the above observations will be useful for the search for further mixed-symmetry phenomena in the neighboring nuclei.

We stress, however, that for the quantitative analysis of the relative proton-neutron symmetry of wave functions it can be more useful to analyze size and isotensor character of electromagnetic transition matrix elements between the calculated states, as was shown above, because of the presence of non-collective states in the shell model configurational space. Considering the radical truncation of the shell model problem which led to the formulation of the IBM it is remarkable how far the IBM and the shell model agree on the properties of mixed-symmetry states of ^{94}Mo .

IV. CONCLUSIONS

To summarize, we have performed shell model calculations for the near-spherical nucleus ^{94}Mo using the Surface Delta Interaction as the residual interaction. We calculated excitation energies of the low-spin positive-parity states and $M1$ and $E2$ transition strengths between them. In most cases the calculations agree well with the data. Calculated wave functions, $M1$, and $E2$ matrix elements support the previous mixed-symmetry assignments for the 1_1^+ state, the 2_3^+ state, and the 3_2^+ state of ^{94}Mo . In particular, we find collective isoscalar $E2$ transitions between these three states and strong isovector $M1$ transitions to low-lying symmetric states. The strongest $M1$ transition is found between the 4_2^+ state and the 4_1^+ state. This transition is outside of the scope of the sd -IBM-2 approach. These findings indicate the common proton-neutron symmetry of the $1_1^+, 2_3^+, 3_2^+$ states showing that they form a class of states that differ to the lowest-lying ones by their proton-neutron structure. The analysis of the wave functions indicates in which neighboring nuclei these states can be most probably found.

V. ACKNOWLEDGMENTS

We thank R.F. Casten, E. Caurier, A. Dewald, L. Esser, A. Gelberg, J. Ginocchio and T. Otsuka for discussions. R.V.J. thanks the Universität zu Köln for a Georg Simon Ohm guest professorship. This work was supported by the *Deutsche Forschungsgemeinschaft* under Contract Nos. Br 799/9-1 and Pi 393/1-1 and one of us (N.P.) got partly support by the US DOE under Contract No. DE-FG02-91ER-40609.

REFERENCES

- [1] N. Pietralla, C. Fransen, D. Belic, P. von Brentano, C. Friessner, U. Kneissl, A. Linneemann, A. Nord, H.H. Pitz, T. Otsuka, I. Schneider, V. Werner, and I. Wiedenhöver, Phys. Rev. Lett. **83**, 1303 (1999).
- [2] N. Pietralla, C. Fransen, P. von Brentano, A. Dewald, A. Fitzler, C. Friessner, and J. Gableske, Phys. Rev. Lett. **84**, 3775 (2000).
- [3] A. Arima, T. Otsuka, F. Iachello, and I. Talmi, Phys. Lett. **B 66**, 205 (1977).
- [4] T. Otsuka, A. Arima, F. Iachello, Nucl. Phys. **A 309**, 1 (1978).
- [5] P. von Brentano, A. Gelberg, H. Harter, and P. Sala, J. Phys. (London) **G 11** L85 (1985).
- [6] T. Otsuka, *Boson model of medium-heavy nuclei*, Ph.D. thesis, University of Tokyo, 1978 (unpublished).
- [7] F. Iachello, Nucl. Phys. **A 358**, 89c (1981); Phys. Rev. Lett. **53**, 1427 (1984).
- [8] A. Faessler, Nucl. Phys. **A85**, 653 (1966).
- [9] A. Faessler and R. Nojarov, Phys. Lett. **166B** 367 (1986).
- [10] R. Nojarov and A. Faessler, J. Phys. G: Nucl. Phys. **13**, 337 (1987).
- [11] N. Lo Iudice and F. Palumbo, Phys. Rev. Lett. **41**, 1532 (1978).
- [12] D. Bohle, A. Richter, W. Steffen, A. E. L. Dieperink, N. LoIudice, F. Palumbo, and O. Scholten, Phys. Lett. **137B** 27 (1984).
- [13] A. Richter, Prog. Part. Nucl. Phys. **34**, 261 (1995), and Refs. therein.
- [14] U. Kneissl, H.H. Pitz, and A. Zilges, Prog. Part. Nucl. Phys. **37**, 349 (1996), and Refs. therein.
- [15] E.L. Johnson, E.M. Baum, D.P. DiPrete, R.A. Gatenby, T. Belgya, D. Wang, J.R. Vanhoy, M.T. McEllistrem, and S. Yates, Phys. Rev. C **52**, 2382 (1995).
- [16] E. Lipparini and S. Stringari, Phys. Lett. **B 130**, 139 (1983).
- [17] D.R. Bes and R. A. Broglia, Phys. Lett. **B 137**, 141 (1984).
- [18] O. Castanos, J.P. Draayer, and Y. Leschber, Ann. Phys. **180**, 290 (1987).
- [19] A. Faessler and R. Nojarov, Phys. Lett. **B 215**, 439 (1988).
- [20] K. Sugaware-Tanabe and A. Arima, Phys. Lett. **B 206**, 573 (1988).
- [21] I. Hamamoto and C. Magnusson, Phys. Lett. **B 260**, 6 (1991).
- [22] G. F. Filippov, A. F. Lisetskyi, and J. P. Draayer, J. Math. Phys. **39**, 1350 (1998).
- [23] C. Rangacharyulu, A. Richter, H.J. Wörtche, W. Ziegler, and R.F. Casten, Phys. Rev. C **43**, R949 (1991).
- [24] N. Pietralla, P. von Brentano, R.-D. Herzberg, U. Kneissl, J. Margraf, H. Maser, H. H. Pitz, and A. Zilges, Phys. Rev. C **52**, R2317 (1995).
- [25] P. von Neumann-Cosel, J.N. Ginocchio, H. Bauer, and A. Richter, Phys. Rev. Lett. **75**, 4178 (1995).
- [26] N. Pietralla, P. von Brentano, R.-D. Herzberg, U. Kneissl, N. LoIudice, H. Maser, H. H. Pitz, and A. Zilges, Phys. Rev. C **58**, 184 (1998).
- [27] W. D. Hamilton, A. Irbäck and J. P. Elliott, Phys. Rev. Lett. **26**, 2469 (1984).
- [28] P. Park, A.R.H. Subber, W. D. Hamilton, J. P. Elliott, and K. Kumar, J. Phys. G: Nucl. Phys. **11**, L251 (1985).
- [29] G. Molnár, R.A. Gatenby, and S.W. Yates, Phys. Rev. C **37**, 898 (1988).
- [30] A. Giannatiempo, A. Nannini, A. Perego, P. Sona, D. Cutoiu, Phys. Rev. C **53**, 2770 (1996).

- [31] W.J. Vermeer, C.S. Lim, R.H. Spear, Phys. Rev. C **38**, 2982 (1988).
- [32] B. Fazekas, T. Belgya, G. Molnár, A. Veres, R.A. Gatenby, S.W. Yates, T. Otsuka, Nucl. Phys. **A548**, 249 (1992).
- [33] J.R. Vanhoy, J.M. Anthony, B.M. Haas, B.H. Benedict, B.T. Meehan, S.F. Hicks, C.M. Davoren, C.L. Lundstedt, Phys. Rev. C **52**, 2387 (1995).
- [34] N. Pietralla, D. Belic, P. von Brentano, C. Fransen, R.-D. Herzberg, U. Kneissl, H. Maser, P. Matschinsky, A. Nord, T. Otsuka, H.H. Pitz, V. Werner, and I. Wiedenhöver, Phys. Rev. C **58**, 796 (1998).
- [35] A. Plastino, R. Arvieu, and S.A. Moszkowski, Phys. Rev. **145**, 837 (1966).
- [36] P. J. Brussard and P. W. M. Glaudemans, *Shell-model applications in nuclear spectroscopy* (North-Holland, Amsterdam, 1977).
- [37] C.M. Lederer, J.M. Jaklevic, and J.M. Hollander, Nucl. Phys. **A169**, 449 (1971).
- [38] D. Zwarts, Comp. Phys. Comm. **38**, 365 (1985).
- [39] E. Caurier, private communication.
- [40] O. Scholten, K. Heyde, P. Van Isacker, J. Jolie, J. Moreau, and M. Warquier, Nucl. Phys. **A438**, 41 (1985).
- [41] H. Liu, and L. Zamick, Phys. Rev. C **36**, 2064 (1987).
- [42] L. Zamick, Phys. Rev. C **31**, 1955 (1985).
- [43] K.-H. Kim, T. Otsuka, P. von Brentano, A. Gelberg, P. Van Isacker, and R.F. Casten, in *Capture Gamma Ray Spectroscopy and Related Topics*, edited by G. Molnár *et al.* (Springer, Budapest, 1996).
- [44] C. Fransen, private communication.

FIGURES

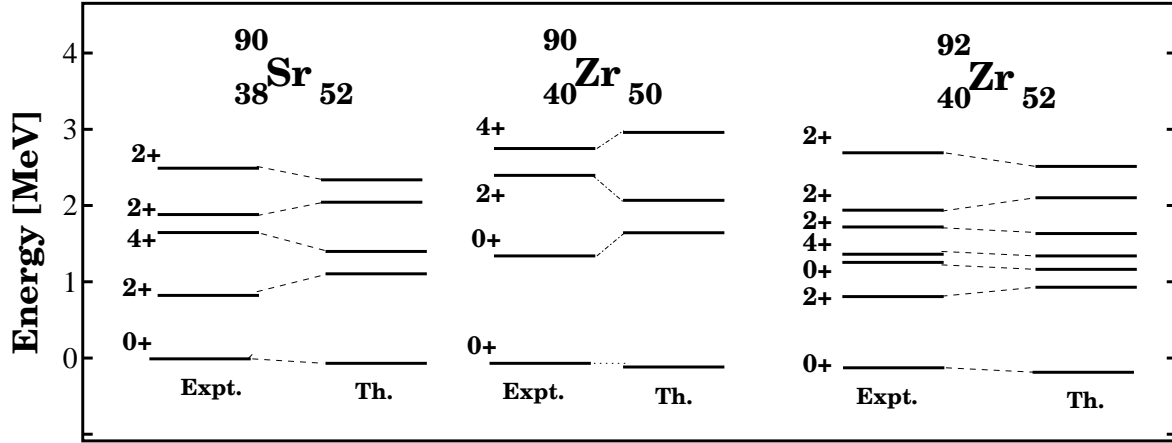


FIG. 1. Calculated and experimental positive parity $J^\pi = 0^+ - 4^+$ states below 3 MeV in ^{90}Sr , ^{90}Zr , and ^{92}Zr .

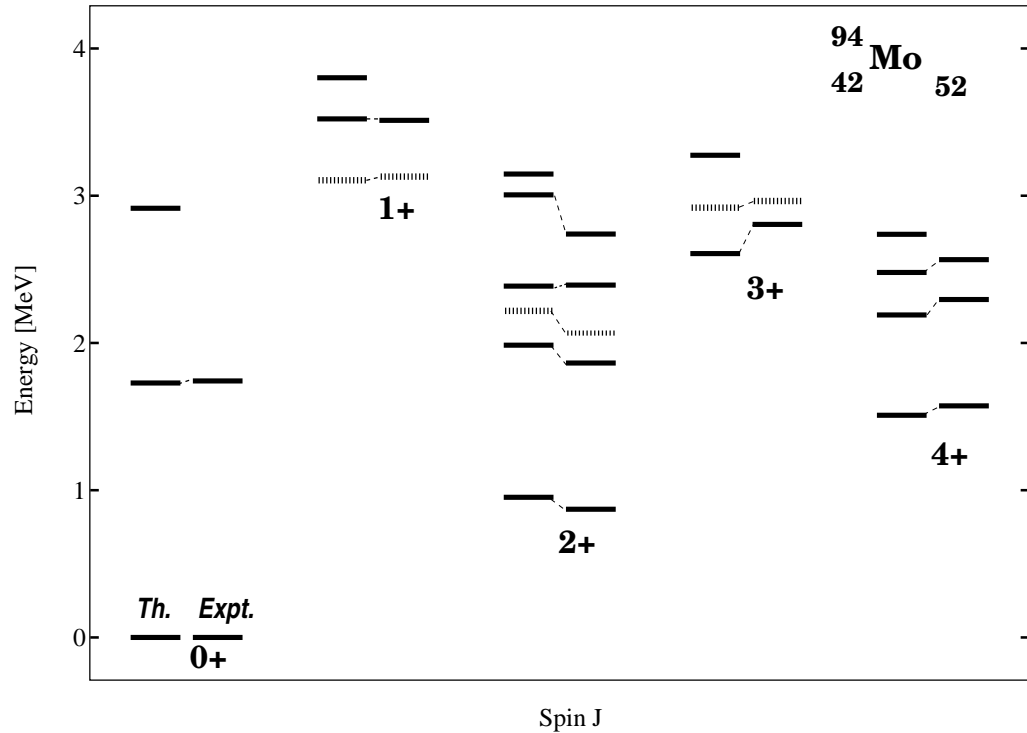


FIG. 2. Comparison of calculated and experimental spectra of the $J^\pi = 0^+ - 4^+$ states in ^{94}Mo . The states with MS assignments are plotted with dashed lines.

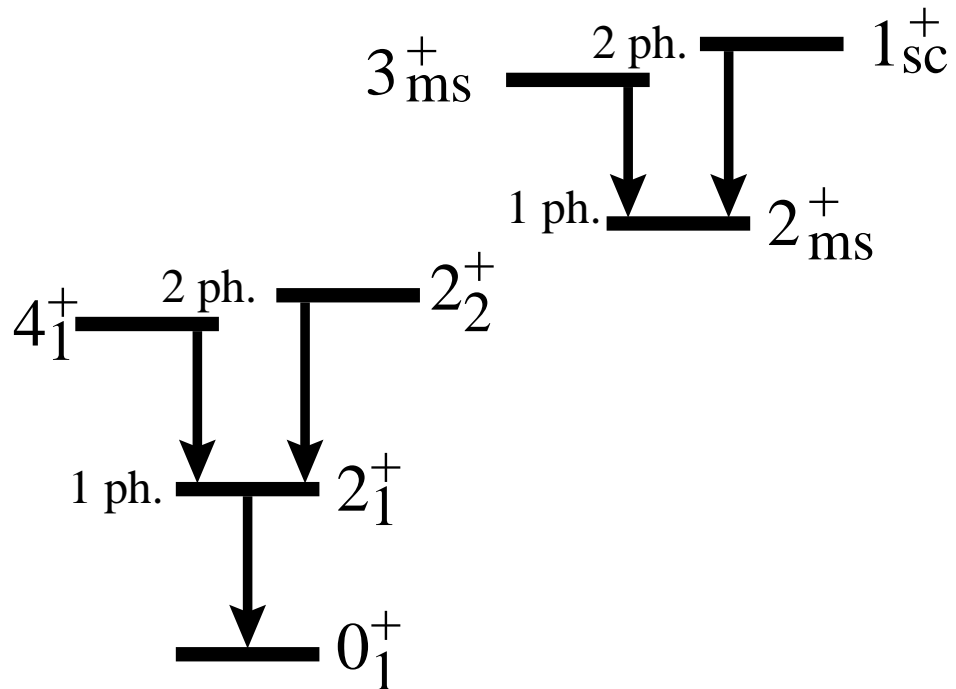


FIG. 3. Sketch of the quadrupole vibrator scheme for low-spin states of ^{94}Mo . The arrows indicate transitions which are expected from this scheme to be collective $E2$ transitions with large isoscalar parts of the matrix elements. The five corresponding values for the isoscalar $E2$ matrix elements which were calculated in the shell model are underlined in Table IV.

TABLES

TABLE I. Parameters used for the shell model calculation of ^{94}Mo : proton and neutron single particle energies for the orbitals included in the configurational space and the interaction parameters of the Surface Delta Interaction as defined in Ref. [36].

| Parameter | $\epsilon_{g_{9/2}}^p$ | $\epsilon_{p_{1/2}}^p$ | $\epsilon_{d_{5/2}}^n$ | $\epsilon_{s_{1/2}}^n$ | $\epsilon_{g_{7/2}}^n$ | $\epsilon_{d_{3/2}}^n$ | $\epsilon_{h_{11/2}}^n$ | $A_{T=1}^{pp}$ | $A_{T=1}^{nn}$ | $A_{T=1}^{pn}$ | $A_{T=0}^{pn}$ |
|-------------|------------------------|------------------------|------------------------|------------------------|------------------------|------------------------|-------------------------|----------------|----------------|----------------|----------------|
| Value [MeV] | 0.0 | -0.8 | 0.0 | 1.4 | 2.0 | 2.2 | 2.4 | 0.31 | 0.24 | 0.27 | 0.50 |

TABLE II. Calculated structure of some low-lying eigenstates of the considered shell model Hamiltonian. The contributions of some low-seniority basis states, which represent for some low-lying states the main components of the wave functions, are shown.

| Component | Component contributions to wave functions (%) | | | | | | | | | | |
|---|---|----------------|---------|---------|---------|---------|---------|---------|---------|---------|---------|
| | State, J_i^π | | | | | | | | | | |
| | 0_1^+ | 0_2^+ | 1_1^+ | 1_2^+ | 2_1^+ | 2_2^+ | 2_3^+ | 3_1^+ | 3_2^+ | 4_1^+ | 4_2^+ |
| $\pi(g_{9/2}^2)_0 \times \nu(d_{5/2}^2)_J$ | 34 | 20 | | | 17 | 3 | 37 | | | 20 | 23 |
| $\pi(p_{1/2}^{-2}g_{9/2}^4)_0 \times \nu(d_{5/2}^2)_J$ | 17 | 21 | | | 8 | 0 | 11 | | | 10 | 12 |
| $\pi(g_{9/2}^2)_J \times \nu(d_{5/2}^2)_0$ | — ^a | — ^a | | | 12 | 23 | 7 | | | 13 | 21 |
| $\pi(p_{1/2}^{-2}g_{9/2}^4)_J \times \nu(d_{5/2}^2)_0$ | — ^a | — ^a | | | 6 | 1 | 7 | | | 6 | 4 |
| $\pi(g_{9/2}^2)_2 \times \nu(d_{5/2}^2)_2$ | 4 | 4 | 25 | 1 | 1 | 11 | 1 | 1 | 21 | 5 | 1 |
| $\pi(p_{1/2}^{-2}g_{9/2}^4)_2 \times \nu(d_{5/2}^2)_2$ | 2 | 6 | 8 | 0 | 0 | 5 | 1 | 0 | 3 | 2 | 0 |
| $\pi(g_{9/2}^2)_4 \times \nu(d_{5/2}^2)_4$ | 1 | 1 | 17 | 0 | 0 | 1 | 0 | 0 | 3 | 0 | 1 |
| $\pi(g_{9/2}^2)_0 \times \nu(d_{5/2}d_{3/2})_J$ | | | 14 | 2 | 0 | 0 | 0 | 0 | 0 | 3 | 0 |
| $\pi(g_{9/2}^2)_0 \times \nu(d_{5/2}g_{7/2})_J$ | | | 3 | 52 | 0 | 0 | 0 | 0 | 0 | 1 | 0 |
| $\pi(g_{9/2}^2)_0 \times \nu(d_{5/2}s_{1/2})_J$ | | | | | 7 | 8 | 0 | 26 | 6 | 0 | 0 |
| $\pi(p_{1/2}^{-2}g_{9/2}^4)_0 \times \nu(d_{5/2}s_{1/2})_J$ | | | | | 4 | 5 | 2 | 12 | 3 | 0 | 0 |
| Components of seniority $\nu = 0$ | 71 | 59 | | | | | | | | | |
| Components of seniority $\nu = 2$ | | | 21 | 54 | 71 | 50 | 73 | 40 | 11 | 65 | 71 |

^asee two lines above

TABLE III. Experimental [1,2] and calculated M1 transition rates between low-lying states of ^{94}Mo . The $B(M1)$ values are given in units of μ_N^2 . Quenched spin g-factors $g_\rho^s = 0.57g_\rho^{s,\text{free}}$ were used in the shell model. Hence, all $M1$ transition strengths shown here are generated by the isovector part of the $M1$ transition operator. Schematic $B(M1)$ values calculated previously [1,2] in the $O(6)$ dynamical symmetry limit of the IBM-2 are given in the last column.

| $J_i \rightarrow J_f$ | $B(M1; J_i \rightarrow J_f) (\mu_N^2)$ | | |
|---------------------------|--|-------------|-------|
| | Experimental | Shell Model | IBM-2 |
| $1_1^+ \rightarrow 0_1^+$ | 0.16(1) | 0.26 | 0.16 |
| $1_2^+ \rightarrow 0_1^+$ | 0.046(18) | 0.008 | 0 |
| $1_1^+ \rightarrow 2_1^+$ | 0.007_{-2}^{+6} | 0.002 | 0 |
| $1_1^+ \rightarrow 2_2^+$ | 0.43(5) | 0.46 | 0.36 |
| $1_1^+ \rightarrow 2_3^+$ | <0.05 | 0.08 | 0 |
| $2_2^+ \rightarrow 2_1^+$ | 0.06(2) | 0.094 | 0 |
| $2_3^+ \rightarrow 2_1^+$ | 0.48(6) | 0.51 | 0.3 |
| $2_4^+ \rightarrow 2_1^+$ | 0.07(2) | 0.01 | 0 |
| $2_5^+ \rightarrow 2_1^+$ | 0.03(1) | 0.14 | 0 |
| $3_2^+ \rightarrow 2_1^+$ | $0.010_{-0.006}^{+0.012}$ | 0.10 | 0 |
| $3_2^+ \rightarrow 4_1^+$ | $0.074_{-0.019}^{+0.044}$ | 0.058 | 0.13 |
| $3_2^+ \rightarrow 2_2^+$ | $0.24_{-0.07}^{+0.14}$ | 0.09 | 0.18 |
| $3_2^+ \rightarrow 2_3^+$ | $0.09_{-0.03}^{+0.07}$ ^a | 0.001 | 0 |
| $4_2^+ \rightarrow 4_1^+$ | 0.8(2) ^b | 1.79 | - |

^a The E2/M1 multipole mixing ratio δ for the $3_2^+ \rightarrow 2_3^+$ transition was not measured unambiguously. For comparison to the SM results we use the smaller value $\delta=0.34(25)$ [2]

^b see Ref. [44]

TABLE IV. Experimental [1,2] and calculated $E2$ transition rates between some low-lying states of ^{94}Mo . The shell model effective neutron and proton charges $e_n = 1.0e$ and $e_p = 2.32e$ were used. The harmonic oscillator length is $b=A^{1/6}$. The schematic IBM-2 estimates [1,2] are given in the fourth column. In columns five and six the total shell model $E2$ matrix elements are decomposed into their isoscalar and isovector parts according to Eqs. (8,9). The underlined values for isoscalar matrix elements represent cases for which collective isoscalar $E2$ transitions are expected from a vibrator model or from the γ -soft dynamical symmetry limits of the IBM.

| $J_i \rightarrow J_f$ | B(E2; $J_i \rightarrow J_f$), [e 2 fm 4] | | | $\langle J_i T_\rho(E2) J_f \rangle$, [efm 2] | |
|---------------------------|--|-------------|-------|--|--------------------------|
| | Experimental | Shell Model | IBM-2 | $\langle T_{IS} \rangle$ | $\langle T_{IV} \rangle$ |
| $2_1^+ \rightarrow 0_1^+$ | 406(16) | 420 | 467 | <u>50.3</u> | -4.6 |
| $2_2^+ \rightarrow 0_1^+$ | 6(2) | 11 | 0 | -0.2 | 7.6 |
| $2_3^+ \rightarrow 0_1^+$ | 46(6) | 42 | 30 | -6.6 | -7.8 |
| $2_4^+ \rightarrow 0_1^+$ | 5(1) | 7.3 | 0 | 2.0 | 4.1 |
| $2_5^+ \rightarrow 0_1^+$ | 17(2) | 8.4 | 0 | 6.0 | 0.5 |
| $4_1^+ \rightarrow 2_1^+$ | 670(100) | 444 | 592 | <u>-69.7</u> | 6.6 |
| $2_2^+ \rightarrow 2_1^+$ | 720(260) | 482 | 592 | <u>49.1</u> | 0 |
| $2_3^+ \rightarrow 2_1^+$ | <150 | 0.03 | 0 | 4.3 | -4.0 |
| $1_1^+ \rightarrow 2_1^+$ | 30(10) | 13 | 49 | 1.5 | 4.8 |
| $1_1^+ \rightarrow 2_2^+$ | — | 1.4 | 0 | -3.7 | 1.7 |
| $1_1^+ \rightarrow 2_3^+$ | <690 | 228 | 556 | <u>25.7</u> | 0.5 |
| $3_2^+ \rightarrow 2_1^+$ | 10_{-9}^{+25} | 43.2 | 48.3 | 5.3 | 12.0 |
| $3_2^+ \rightarrow 4_1^+$ | < 17.8 | 23 | 0 | -12.8 | 0.1 |
| $3_2^+ \rightarrow 2_2^+$ | <101.6 | 170.2 | 0 | -39.3 | 4.8 |
| $3_2^+ \rightarrow 2_3^+$ | 254_{-203}^{+305} a | 198.2 | 582 | <u>42.5</u> | -5.3 |

^asee footnote “a” of Table III